

PDF hosted at the Radboud Repository of the Radboud University Nijmegen

The following full text is a publisher's version.

For additional information about this publication click this link.

<http://hdl.handle.net/2066/98849>

Please be advised that this information was generated on 2017-12-06 and may be subject to change.

Size and charge effects on the binding of CO to late transition metal clusters

André Fielicke,^{a)} Gert von Helden, and Gerard Meijer

Fritz-Haber-Institut der Max-Planck-Gesellschaft, Faradayweg 4-6, D-14195 Berlin, Germany

David B. Pedersen,^{b)} Benoit Simard, and David M. Rayner^{c)}

Steacie Institute for Molecular Sciences, National Research Council, 100 Sussex Drive, Ottawa, Ontario K1A 0R6, Canada

(Received 6 February 2006; accepted 23 March 2006; published online 16 May 2006)

We report on the size and charge dependence of the C–O stretching frequency, $\nu(\text{CO})$, in complexes of CO with gas phase anionic, neutral, and cationic cobalt clusters ($\text{Co}_n\text{CO}^{-/0/+}$), anionic, neutral, and cationic rhodium clusters ($\text{Rh}_n\text{CO}^{-/0/+}$), and cationic nickel clusters (Ni_nCO^+) for n up to 37. We develop models, based on the established vibrational spectroscopy of organometallic carbonyl compounds, to understand how cluster size and charge relate to $\nu(\text{CO})$ in these complexes. The dominating factor is the available electron density for backdonation from the metal to the CO π^* orbital. Electrostatic effects play a significant but minor role. For the charged clusters, the size trends are related to the dilution of the charge density at the binding site on the cluster as n increases. At large n , $\nu(\text{CO})$ approaches asymptotes that are not the same as found for $\nu(\text{CO})$ on the single crystal metal surfaces, reflecting differences between binding sites on medium sized clusters and the more highly coordinated metal surface sites. © 2006 American Institute of Physics.

[DOI: [10.1063/1.2196887](https://doi.org/10.1063/1.2196887)]

I. INTRODUCTION

Carbon monoxide is an important ligand in organometallic, surface, and cluster science. Its interactions with bulk and finite metal systems have been studied extensively, both because of the intrinsic interest in its chemistry on surfaces, especially that related to heterogeneous catalysis, and because it can be used to probe structure and charge in supported transition metal atoms and nanoparticles. A main attraction of CO for experimental studies is that the C–O stretching frequency, $\nu(\text{CO})$, is highly sensitive to the nature of the binding site and to the electron density. The infrared (IR) spectroscopy of adsorbed CO has long been used to characterize binding sites and cluster-support interactions of metals such as rhodium dispersed on amorphous metal oxide supports.¹ The approach is now being applied to study the structure and chemistry of size-selected transition metal nanoparticles following the development of methods to investigate deposited clusters of known size. Such techniques include size-selective deposition^{2,3} and postdeposition characterization by scanning probe microscopy.^{4–7}

We are pursuing infrared spectroscopy studies of isolated metal cluster-carbonyl complexes in the gas phase to extend the understanding of metal-ligand interactions in general, to characterize how the properties of cluster surfaces differ from and evolve toward the bulk surface properties, to develop methods for following chemical reactions on cluster surfaces and, more specifically, to provide a more secure

foundation for interpreting CO probes of supported clusters. How the effects of structure, size, and charge on the binding of CO to the clusters are reflected in the $\nu(\text{CO})$ frequencies provides a baseline to identify and quantify support effects. For instance, the amount of charge transferred to the support can be estimated if $\nu(\text{CO})$ can be compared in equivalent free and supported clusters. Until recently, the interpretation of the vibrational spectra of CO adsorbed on supported metal species relied on comparison with $\nu(\text{CO})$ values of stable, molecular metal carbonyl compounds, of CO adsorbed on single crystal surfaces, and of atom-CO complexes in rare gas matrices.

The infrared spectroscopy of gas phase metal cluster complexes has recently gained highly from the introduction of the free electron laser (FEL) as a light source for resonance enhanced infrared multiple photon excitation spectroscopy.⁸ Using an IR-FEL it becomes possible to access internal vibrational modes of the adsorbed ligand,^{9–15} modes associated with the ligand-cluster bond,¹² and modes of the cluster itself.^{16,17} The adsorbed ligand and ligand-cluster modes provide information on the cluster-ligand interaction. They can characterize the binding site and can identify changes occurring in the ligand on adsorption. The measurement of the vibrational modes of the cluster, in conjunction with density functional theory (DFT) calculations, provides valuable information on the structure of the cluster itself.

In the study reported here we use IR multiple photon dissociation (IR-MPD) spectroscopy to investigate the size evolution of CO bonding in cluster complexes of the late transition metals cobalt, rhodium, and nickel containing up to 37 metal atoms. By measuring the vibrational spectra of

^{a)}Electronic mail: fielicke@fhi-berlin.mpg.de

^{b)}Present address: Chemical and Biological Defense, DRDC Suffield, P.O. Box 4000 Station Main, Medicine Hat, AB T1A 8K6, Canada.

^{c)}Electronic mail: david.rayner@nrc-cnrc.gc.ca

CO adsorbed on anionic, cationic, and neutral clusters we probe the influence of the charge on the CO binding and provide a calibration for $\nu(\text{CO})$ as a function of charge and cluster size. We concentrate here on complexes with single CO molecules occupying atop (μ^1) sites. Our early work on rhodium cluster complexes, $\text{Rh}_n\text{CO}^{-/0/+}$, with $n \leq 15$, identified this as the predominant mode of binding.^{10,11} All rhodium clusters with $n > 4$ show μ^1 binding with a few clusters in the range of $n = 5 - 14$ also showing coexisting, but never dominant bridge bound, μ^2 complexes. We present new results on Rh clusters for $n = 16 - 34$ in addition to a complete study of anionic, neutral, and cationic Co clusters up to $n = 37$ and a study of cationic Ni clusters up to $n = 23$. In all the complexes the dominant mode of binding remains atop. From the results for the three systems we develop a general understanding of the roles of electrostatic effects and of π^* backbonding in determining $\nu(\text{CO})$ and how those effects evolve with cluster size.

II. EXPERIMENT

The experiments are performed using a molecular beam apparatus coupled to the beamline of the Free Electron Laser for Infrared eXperiments (FELIX).^{8,18} The use of FELIX for IR spectroscopy of metal clusters, metal compound clusters, and cluster-ligand complexes has been described in parts earlier.⁸⁻¹⁰ The details of the present experiment are the same as those described for our work on the smaller $\text{Rh}_n\text{CO}^{-/0/+}$ complexes.¹¹ Briefly neutral, cationic, and anionic metal clusters are produced in a pulsed laser vaporization source and entrained in a flow of He. They pick up CO, delivered through a second pulsed valve, in a small reactor channel before expanding to produce a beam containing cluster-CO complexes. The extent of CO complex formation is controlled by adjusting the CO flow through the second valve. The beam passes through a skimmer to the detection chamber, where the complexes are detected using a pulsed-field-extraction time-of-flight mass spectrometer (TOFMS). The IR beam counter propagates with respect to the cluster beam and is loosely focused to fill an aperture through which the cluster beam enters the ion detection region of the TOFMS. This ensures that the full cross section of the cluster beam entering the TOFMS is exposed to the IR laser beam. To study neutral complexes charged deflection plates are placed just before the aperture to remove ionic species from the beam. The neutral species are subsequently ionized between the extraction plates of the mass spectrometer using an excimer laser run on F_2 (157 nm), with the laser fluence kept sufficiently low to avoid fragmentation induced by UV multiphoton absorption. For the detection of the anions, all voltages of the mass spectrometer are reversed.

FELIX delivers macropulses of infrared radiation of 6–8 μs duration at a repetition rate of 5 Hz. The wavelength can be continuously tuned throughout the 3–250 μm region, although for the experiments reported here only the 4.5–6.0 range is used. Each macropulse consists of a 1 GHz train of micropulses of typically 2 ps duration. The macropulse energy was 7 mJ at 2000 cm^{-1} corresponding to a micropulse energy of $\sim 1 \mu\text{J}$. In the $\nu(\text{CO})$ stretching region FELIX

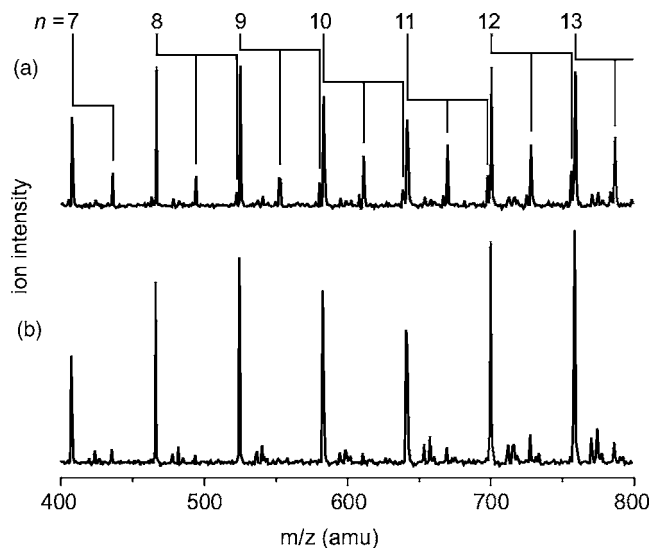


FIG. 1. Mass spectra demonstrating IR multiple photon dissociation of cationic cobalt cluster-CO complexes, $\text{Co}_n(\text{CO})_m^+$. Spectrum (a) is obtained with the IR laser tuned to 1900 cm^{-1} , out of resonance with any IR band of the cationic complexes. Peaks due to $\text{Co}_n(\text{CO})_1^+$ and $\text{Co}_n(\text{CO})_2^+$ are identified by vertical bars. The spectrum is identical to that obtained with the IR laser turned off. Spectrum (b) is obtained with the IR laser tuned to 2000 cm^{-1} , in resonance with the CO stretching frequency, $\nu(\text{CO})$, for many of the CO complexes in this mass range. Strong depletion of the $\text{Co}_n(\text{CO})_m^+$ mass peaks and growth of the bare Co_n^+ cluster peaks is apparent.

frequencies are calibrated by recording the infrared absorption spectra of ethylene and CO in a photoacoustic cell. The bandwidth of the IR laser radiation is measured on the Q branch of the $\nu_7 + \nu_8$ combination band of ethylene to be 10–20 cm^{-1} at 1890 cm^{-1} .

The TOFMS extraction pulse is timed to collect ions from the portion of the beam exposed to FELIX. Infrared spectra are constructed from mass spectra that are recorded as the FELIX wavelength is scanned incrementally. Reference mass spectra, with the IR pulse turned off, are recorded on alternate shots to compensate for drift in the cluster beam intensity. The IR depletion spectra are subsequently constructed by integration over the mass spectral signal intensity corresponding to a certain complex and normalization with the intensity of the nonirradiated reference distribution for each wavelength.

III. RESULTS

A. Cobalt cluster-CO complexes

The resonant IR-MPD of metal cluster-CO complexes in the CO stretching region of the spectrum is demonstrated in Fig. 1 using cationic Co cluster complexes as an example. When the IR radiation is resonant with $\nu(\text{CO})$, full depletion of the CO complexes is observed. Typical photodepletion spectra of anionic, neutral, and cationic cobalt cluster-monocarbonyl clusters, $\text{Co}_n\text{CO}^{-/0/+}$, as constructed from such mass spectra taken at regular wavelength intervals, are shown in Fig. 2 for $n = 8$ and $n = 17$. Several features are apparent in these spectra that turn out to be general for the late transition metals. $\nu(\text{CO})$ is clearly sensitive to the charge on the cluster, the cations absorbing at higher energy than the neutrals that in turn absorb to the blue of the anions. The

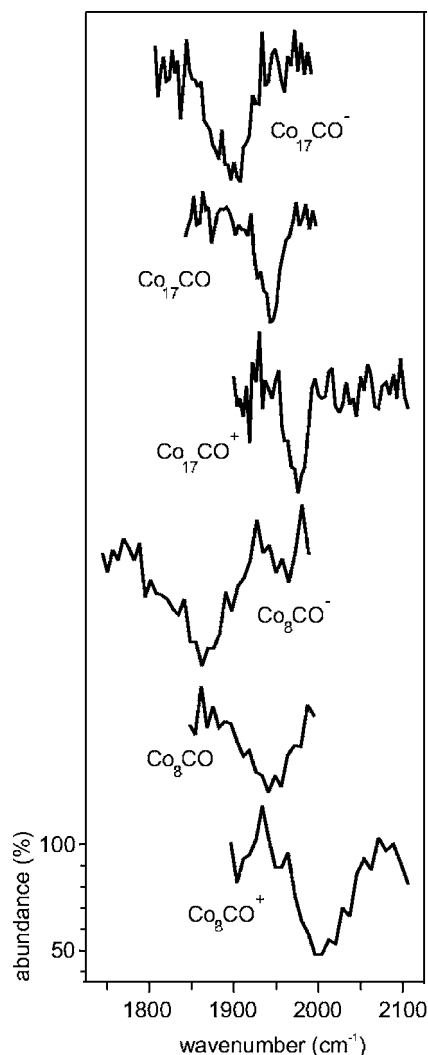


FIG. 2. IR multiple photon depletion spectra of anionic, neutral, and cationic cobalt cluster-CO complexes, $\text{Co}_n\text{CO}^{-/0/+}$, with $n=8$ and $n=17$. The spectra are offset for clarity and are all plotted on the same relative abundance scale.

effect of charge is greater for the smaller clusters. In the neutral cluster $\nu(\text{CO})$ is largely insensitive to cluster size. These features hold over the cluster size range studied, as shown in Fig. 3, where $\nu(\text{CO})$ is plotted as a function of cluster size for all three charge states of Co_nCO .

Taking the charge state dependence into account, as discussed below, the reported frequencies are all consistent with CO binding in an atop, μ^1 , fashion toward a single Co atom. In the case of rhodium cluster-CO complexes, $\text{Rh}_n\text{CO}^{-/0/+}$, CO is predominantly bridge bound only in certain small complexes, i.e., Rh_3CO^+ (μ^2), Rh_4CO^+ (μ^3), and Rh_4CO (μ^3).¹¹ For a few cluster sizes in the range $n=5-14$, complexes with μ^2 bridge bound CO coexist with μ^1 bound CO complexes. We were not able to determine if this is due to the availability of two isoenergetic binding configurations on a single Rh_n structure or to the presence of more than one cluster isomer in the molecular beam. In the case of Co clusters there is no evidence for bridge binding in any of the complexes studied. Achievable cluster beam distributions prevented us from measuring most small clusters in the size range $n \leq 4$, where the Rh clusters show predominant bridge

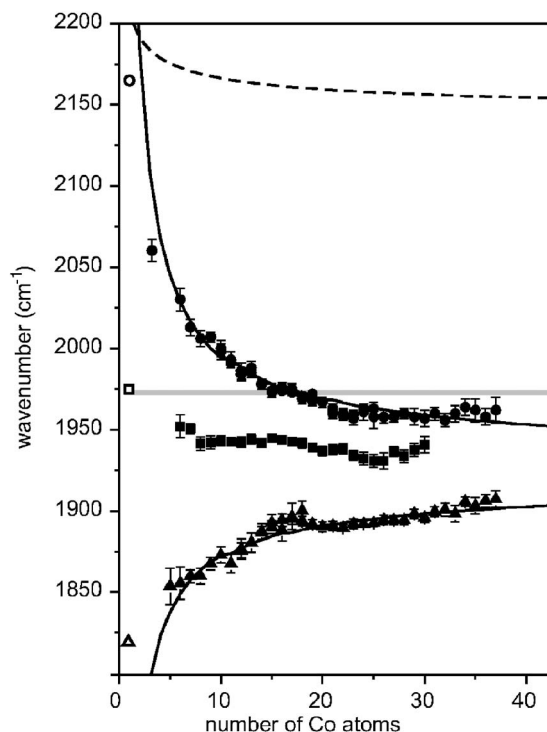


FIG. 3. Frequency of the $\nu(\text{CO})$ vibration of atop CO in Co_nCO cations (\bullet), neutrals (\blacksquare), and anions (\blacktriangle) as a function of cluster size. The peak positions are determined by a least-squares fit to a Gaussian peak shape. The error bars represent the standard deviation (1σ) of the fit. The values of $\nu(\text{CO})$ in the atomic complexes $\text{CoCO}^{-/0/+}$ measured in Ne matrices from Ref. 29 are indicated by open symbols. The dashed line represents the contribution of the electrostatic effect for a positive charged cluster, while the continuous lines are obtained from the model that includes electrostatic effect and π backdonation. The gray line marks $\nu(\text{CO})$ for CO adsorbed on a $\text{Co}(10\bar{1}0)$ surface (Ref. 34).

binding. The exception is Co_3CO^+ . For this complex and the larger $\text{Co}_n\text{CO}^{-/0/+}$ complexes with $n \geq 5$ studied here, the ability to saturate the depletion through excitation at the frequency of the vibrational band attributed to μ^1 bound CO indicates that bridge bound complex isomers are not formed in significant quantities. Taking signal-to-noise considerations into account we estimate that bridge bound complexes can only be present as minority species at $<20\%$ of the μ^1 concentration.

A final feature of the spectra shown in Fig. 2 is that, irrespective of charge state, the smaller cluster complexes with $n=8$ have appreciably broader $\nu(\text{CO})$ bands than the larger complexes with $n=17$. The reason for this is not clear. It could reflect the availability of well defined lowest energy binding sites of similar coordination on the larger clusters, whereas the smaller clusters may have more than one μ^1 binding site with similar energetics but slightly different $\nu(\text{CO})$. It is also possible that the broadening for the smaller clusters is linked to the IR-MPD process itself; the smaller clusters required more IR intensity to show depletion. We do not pursue this further in this paper, but rather focus on the effect of charge and size on $\nu(\text{CO})$ that is well determined in either case.

B. Larger rhodium cluster-CO complexes

We have already reported the values of $\nu(\text{CO})$ for anionic, neutral, and cationic rhodium cluster-CO complexes,

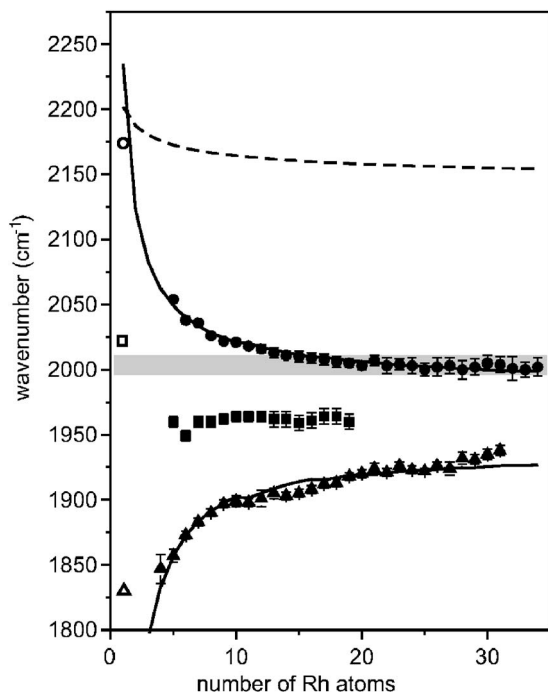


FIG. 4. Frequency of the $\nu(\text{CO})$ vibration of atop CO in Rh_nCO cations (●), neutrals (■), and anions (▲) as a function of cluster size. The peak positions are determined by a least-squares fit to a Gaussian peak shape. The error bars represent the standard deviation (1σ) of the fit. The values of $\nu(\text{CO})$ in the atomic complexes $\text{RhCO}^{-/0/+}$ measured in Ne matrices from Ref. 29 are indicated by open symbols. The dashed line represents the contribution of the electrostatic effect for a positive charged cluster, while the continuous lines are obtained by including electrostatic effect and π back donation in the model. The gray band marks the range of the values reported for $\nu(\text{CO})$ μ^1 bound on Rh(111), (110), and (100) surfaces (Refs. 35–38).

$\text{Rh}_n\text{CO}^{-/0/+}$, over the size range $n=3-15$.^{10,11} Here, this range is extended up to $n=34, 19,$ and 31 for the cationic, neutral, and anionic complexes, respectively. The results are shown in Fig. 4 together with the values of $\nu(\text{CO})$ for μ^1 bound CO from the earlier study. For $n=15$ and above we find no evidence for bridge bound CO, although, again, noise could mask the presence of small quantities of such complexes.

C. Nickel cluster-CO complexes

IR photodepletion spectra of cationic nickel cluster-monocarbonyl clusters are shown in Fig. 5. Again they show a single band attributable to atop bound CO that shifts to the red with increasing cluster size. Figure 6 reports the cluster size dependence of $\nu(\text{CO})$ for Ni_nCO^+ complexes from $n=4$ to $n=23$.

IV. CHARGE AND SIZE DEPENDENCE OF $\nu(\text{CO})$

In organometallic chemistry, the long established, classical picture of the bonding between a transition metal atom and carbon monoxide includes both $M\leftarrow C$ σ bonding and $M\rightarrow C$ π backbonding. The $M\leftarrow C$ σ bonding involves donation from the $\text{CO}(5\sigma)$ orbital into a suitable acceptor orbital on the metal atom. The $M\rightarrow C$ π backbonding involves donation from a metal d orbital into the $\text{CO}(2\pi^*)$ antibonding orbital. This picture was adopted early on to describe CO

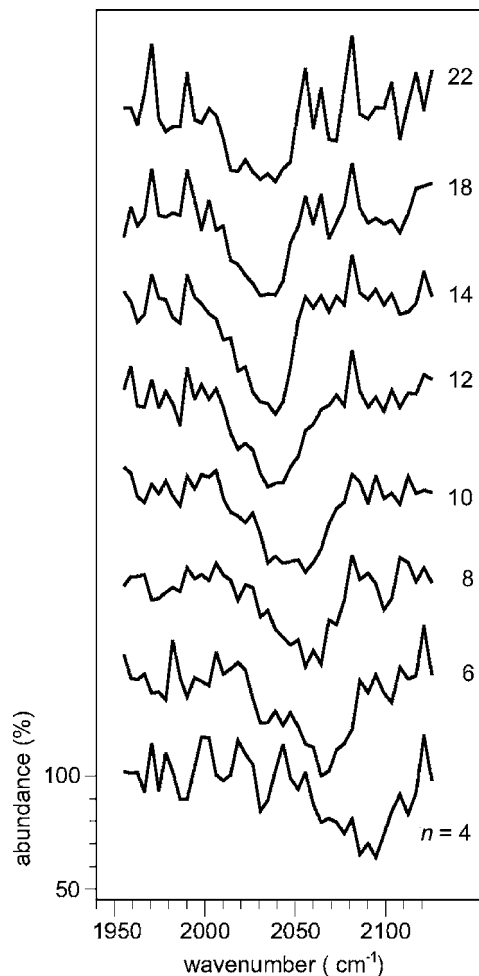


FIG. 5. IR multiple photon depletion spectra of cationic nickel cluster-CO complexes, Ni_nCO^+ , in the range $n=4-22$. The spectra are offset for clarity.

interactions with metal surfaces,¹⁹ where it is in acceptable use,²⁰ and is adopted as the basis for discussing CO adsorption to metal clusters from a molecular orbital viewpoint.²¹ In extended transition metal systems $M(sp)$ hybrid orbitals may also contribute to the $M\rightarrow C$ π backbonding.

The C–O stretching frequency is related to the strength of the C–O bond and therefore to the magnitudes of $M\rightarrow C$

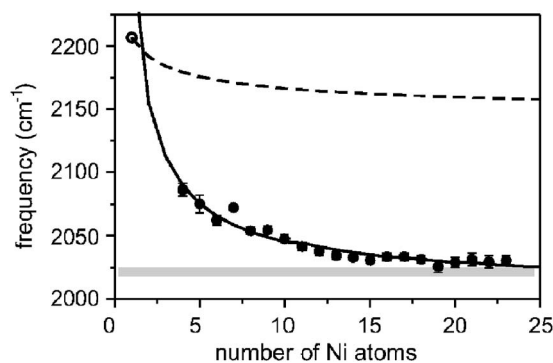


FIG. 6. Frequency of the $\nu(\text{CO})$ vibration of atop CO in Ni_nCO cations (●) as a function of cluster size. The peak positions are determined by a least-squares fit to a Gaussian peak shape. The error bars represent the standard deviation (1σ) of the fit. The gray line marks $\nu(\text{CO})$ for CO adsorbed at μ^1 sites on Ni(100) and Ni(119) (Refs. 31 and 39). The open circle indicates the value of $\nu(\text{CO})$ for NiCO^+ in a Ne matrix (Ref. 29).

π backbonding and $M \leftarrow C$ σ bonding. It is accepted that π backdonation weakens the C–O bond and results in a decrease in $\nu(\text{CO})$, while the $M \leftarrow C$ donation does the opposite and increases $\nu(\text{CO})$, albeit to a lesser extent. This argumentation originated in a molecular orbital analysis that found the 5σ orbital in free CO to be antibonding with regard to the C–O coordinate. In the so-called nonclassical CO metal complexes that have carbonyl frequencies as much as 100 cm^{-1} higher than that of free CO on the other hand, the predominance of $M \leftarrow C$ σ bonding over $M \rightarrow C$ π backbonding was postulated to explain the high values of $\nu(\text{CO})$. More recently it has been proposed that the degree of $M \leftarrow C$ σ bonding has little direct effect in raising $\nu(\text{CO})$. Higher level, basis set independent Hartree-Fock *ab initio* calculations contradict the molecular orbital results and show that the 5σ orbital in free CO is, if anything, bonding with regard to the C–O coordinate.²² Rather, the high values of $\nu(\text{CO})$ in the nonclassical CO metal complexes could be shown to be due to electrostatic effects related to the cationic metal centers encountered in these complexes.^{22,23} The general conclusion from these and other arguments is that $M \leftarrow C$ σ bonding plays no major role in determining $\nu(\text{CO})$ in transition metal carbonyls in general.²³ Note that this does not mean that σ bonding is unimportant, but only that $\nu(\text{CO})$ is relatively insensitive to it.

The electrostatic effect is due to the interaction of the electric field of the charged metal center with the C–O bonding orbitals. In free CO these orbitals are polarized toward oxygen. For positively charged ions the field opposes this polarization, moving the charge into the bond and increasing the covalency. Classically, the field exerts a force between the partially positively charged C atom and the partially negatively charged O atom that pulls them together, increasing the force constant associated with the bond. Quantum mechanical calculations on model systems and on nonclassical carbonyls reinforce this picture.^{22,23}

A quantitative framework for evaluating $\nu(\text{CO})$ follows from early studies that established a linear relationship between calculated CO $2\pi^*$ orbital populations and experimental frequencies in metal carbonyl compounds.^{24,25} Under the assumption that the effect of σ bonding is not significant, as discussed above, extension of this approach to include the change induced by the electrostatic effect, ΔF_{ES} , gives the C–O stretching force constant F_{CO} as follows:

$$F_{\text{CO}} = F_{\text{free}} + \Delta F_{\text{ES}} - \beta P(2\pi), \quad (1)$$

where F_{free} is the C–O stretch force constant in free CO, ΔF_{ES} is the change in F_{free} due to the electrostatic effect, $P(2\pi)$ is the CO $2\pi^*$ orbital population, and β is a coefficient related to the strength of the effect of $2\pi^*$ occupation on $\nu(\text{CO})$.²³ To relate $\nu(\text{CO})$ to F_{CO} we adopt the energy factoring approximation²⁶ equating F_{CO} with the stretching parameter k_{CO} , so that

$$\nu(\text{CO}) = \frac{1}{2\pi} \sqrt{\frac{F_{\text{CO}}}{\mu_{\text{CO}}}}. \quad (2)$$

Our first step is to gauge the importance of the electrostatic effect. To do this we borrow from the *ab initio*

quantum mechanical analysis of the effect in metal carbonyl compounds. Goldman and Krough-Jespersen²³ have calculated the dependence of F_{CO} on the field due to a point charge placed at various distances from the carbon end of CO. Their results show ΔF_{ES} to be proportional to the electric field E over the range of interest, with $\Delta F_{\text{ES}} = 24.98 \text{ m dyn } \text{Å}^{-1} \times E/\text{a.u.}$ This shift is positive for a positively charged metal center. A very similar number is obtained from the results of an independent calculation by Lupinetti *et al.*²² Substituting $F_0 + \Delta F$ for F_{CO} in Eq. (2), under the condition $\Delta F \ll F_0$, the *ab initio* results lead to

$$\Delta \nu_{\text{ES}} = 1395 \text{ cm}^{-1} \times E/\text{a.u.} \quad (3)$$

For metal carbonyl complexes the field is determined as z/r^2 , where z is the charge on the metal atom and $r = r_{M-C} + r_{C-O}/2$, the distance from the metal atom to the center of the C–O bond. Calculations have not been performed for anionic complexes and we assume that Eq. (3) holds with the sign of the field reversed when z is negative. For metal cluster complexes we start with the postulation that the clusters are sufficiently metallic for the charge to be distributed over the surface atoms. To provide a simple, structure independent model we treat the clusters as conducting spheres so that the field at r is still given by z/r^2 , where r is now the distance from the center of the cluster to the center of the C–O bond. We have tested this approach by calculating the field explicitly for representative metal cluster structures obtained from theory,^{27,28} with the charge distributed over the surface atoms. The conducting sphere approximation somewhat overestimates $\Delta \nu_{\text{ES}}$ for the smaller clusters, but the differences are not significant ($< 5 \text{ cm}^{-1}$).

To estimate the cluster size we set $r = (r_{\text{CL}} + r_{\text{C}} + r_{\text{C-O}})/2$, where r_{CL} is the cluster radius and r_{C} is the covalent radius of the carbon atom in a typical $M-C$ bond. We approximate $r_{\text{CL}} \approx r_{\text{M}} n^{1/3}$, where r_{M} is the classical radius of the atom as obtained from the bulk density.

In Figs. 3, 4, and 6 we compare the predicted evolution of $\nu(\text{CO})$ with n due to the electrostatic effect with the experimental $\nu(\text{CO})$ for the cationic ($z = +1$) Co, Rh, and Ni cluster complexes. r_{M} is taken as 2.62, 2.81, and 2.61 bohr (1.39, 1.48, and 1.38 Å) for cobalt, rhodium, and nickel, respectively, and we use 0.98 bohr (0.52 Å) for r_{C} and 2.18 bohr (1.15 Å) for $r_{\text{C-O}}$. The calculated frequencies shown by the dashed lines in the figures assume no π backbonding and are obtained as $\nu_{\text{free}} + \Delta \nu_{\text{ES}}$ ($\nu_{\text{free}} = 2143 \text{ cm}^{-1}$). It is seen from the figures that the electrostatic effect, although significant, only plays a minor role in determining $\nu(\text{CO})$. For cobalt, over the range $n = 6-37$ the electrostatic effect only predicts a change of 18 cm^{-1} compared to the experimental drop of 60 cm^{-1} and very similar results are obtained for the other metals.

To include π backdonation into the model we return to Eq. (1) and postulate that the change in the $2\pi^*$ orbital population due to the charge on the cluster, $\Delta P(2\pi)$, is proportional to the partial charge on the binding site atom. The implication of our earlier assumption that the ion charge is distributed over the cluster surface is that the effective partial charge at the binding site is inversely proportional to the

TABLE I. Values of ν_∞ (cm⁻¹), γ' (cm⁻¹), and $\beta\gamma$ (mdyn Å⁻¹) found by fitting the cluster size dependence of $\nu(\text{CO})$ using Eq. (7).

Metal	Anion			Neutral	Anion			Surface ^a ν_{surf}
	ν_∞	γ'	$\beta\gamma$		ν_∞	γ'	$\beta\gamma$	
Co	1922	-258	6.7	1940	1930	403	4.0	1972 ^b
Rh	1934	-536	3.0	1960	1980	191	8.4	1995–2015 ^c
Ni					2002	221	3.6	2020 ^d

^aValues taken from the literature for μ^1 sites occupied at low CO coverage.

^bFor Co(10 $\bar{1}$ 0) from Ref. 34.

^cRange of the values for Rh(111), (110), and (100) from Refs. 35–38.

^dFor Ni(100) and Ni(119) step sites from Refs. 31 and 39.

number of surface atoms, n_S . This leaves $\Delta P(2\pi)$ proportional to z/n_S and the orbital population can be written as follows:

$$P(2\pi) = P(2\pi)_\infty - \Delta P(2\pi) = P(2\pi)_\infty - \frac{\gamma z}{n_S}, \quad (4)$$

where γ is the proportionality constant. The C–O stretching force constant is then given by

$$F_{\text{CO}} = F_{\text{free}} + \Delta F_{\text{ES}} - \beta \left(P(2\pi)_\infty - \frac{\gamma z}{n_S} \right), \quad (5)$$

which can be written as

$$F_{\text{CO}} = F_\infty + \Delta F_{\text{ES}} + \frac{\beta \gamma z}{n_S}, \quad (6)$$

where F_∞ is the asymptotic value of F_{CO} as n_S tends to infinity. Transforming this to frequencies with $\gamma' = \nu_\infty \beta \gamma z / 2F_\infty$ gives

$$\nu(\text{CO}) = \nu_\infty + \Delta \nu_{\text{ES}} + \frac{\gamma'}{n_S}. \quad (7)$$

In the large cluster limit we expect n_S to be proportional to the surface area and therefore to $n^{2/3}$. This does not hold for the smaller clusters in our sample and, instead, we estimate n_S from what is known of the close-packed compact structures of late transition metal clusters. Taking Ni_{*n*} clusters to be representative we derive, from their known structures in the size range $n=1-55$ (Ref. 21), the empirical relationship $n_S = 1.29n^{0.873}$. $\Delta \nu_{\text{ES}}$ depends on n but can be calculated from the field using Eq. (3), allowing us to fit the experimental frequencies as a test of the model and to obtain ν_∞ and γ' . The fitted frequencies for the cobalt and rhodium cationic and anionic complexes and for the nickel cationic complexes are shown as the solid lines in Figs. 3, 4, and 6, and the fitting parameters ν_∞ and γ' are given in Table I. Considering the crudeness of the model, the agreement is very good and it is remarkable that even the independently obtained results for $\nu(\text{CO})$ in the monocarbonyls CoCO^{+/-} and RhCO^{+/-} in neon matrices²⁹ (not included in the fits) lie close to the predicted values.

From the above we conclude that the size and charge dependences of $\nu(\text{CO})$ in the late transition metal cluster-CO complexes studied here can be understood in terms of charge dilution as the cluster size increases. Charge dilution lowers $\nu(\text{CO})$ in cationic clusters and raises it in anionic clusters

because of the role both the electrostatic effects and π^* backbonding play in determining $\nu(\text{CO})$ in these complexes. The electrostatic effect is more important for small clusters, but over most of the cluster size ranges studied here the dependence of π^* backbonding on the local electron density at the single-atom binding site accounts for the large part of the size dependence.

The global success of the model does not rule out the possibility of some localization of charge at the binding site. Indeed, such residual localization may explain why the asymptotes ν_∞ for the charged complexes do not always coincide exactly with the neutral values (Table I). Variations in this localization, along with slight differences in orbital overlap, may also explain the small local deviations in $\nu(\text{CO})$ from the fully delocalized model evident in Figs. 3, 4, and 6.

In the neutral complexes $\nu(\text{CO})$ is largely independent of cluster size, varying by only ± 10 cm⁻¹ over the size ranges studied. Of course the charge effect models predict no dependence of $\nu(\text{CO})$ on size in neutral cluster complexes. The invariance of $\nu(\text{CO})$ with cluster size implies that clusters up to at least $n=30$ in the case of Co_{*n*} and $n=19$ in the case of Rh_{*n*} have available at least one similar lowest energy μ^1 binding site.

Also listed in Table I is the product $\beta\gamma$ calculated from the fitting parameters ν_∞ and γ' . The coefficient β relates the population of the CO $2\pi^*$ orbital to the CO force constant [Eq. (1)]. γ can be interpreted as the fraction of available charge that is transferred to the CO $2\pi^*$ orbital. If we take $\gamma=1$ we find β in the range 3.0–8.4 mdyn Å⁻¹. These values can be compared to those found from force constants obtained from *ab initio* calculations on organometallic carbonyl compounds,²³ where $\beta \sim 4$ mdyn Å⁻¹ was found from intermolecular comparisons and somewhat higher values in the range 8–12 mdyn Å⁻¹ were found from intramolecular comparisons. The fact that our model returns similar values of β argues that we have made a reasonable description of π backbonding as it effects $\nu(\text{CO})$ in charged metal cluster-CO complexes.

V. COMPARISON WITH CO ADSORBED ON SURFACES AND SUPPORTED NANOPARTICLES

Reported values of $\nu(\text{CO})$ for CO μ^1 bound on cobalt, rhodium, and nickel surfaces at low coverage are given in Table I and are shown by the grey lines in Figs. 3, 4, and 6. In all cases the surface $\nu(\text{CO})$ is at higher frequency than the respective ν_∞ asymptotes of even the cationic clusters. Over the size range studied here the charged complexes have $\nu(\text{CO})$ that tends to values close to, in the case of cobalt, or at least span, in the case of rhodium, the relatively invariant values shown by the neutral clusters.

In the neutral complexes $\nu(\text{CO})$ values are found to be 40–50 cm⁻¹ below the respective surface values. We associate the redshift in $\nu(\text{CO})$ with the availability of lower metal-coordinated atom sites for atop adsorption on cluster surfaces as compared to single crystal surfaces. More available charge at low coordinated binding sites and, perhaps, more favorable orbital overlap can lead to increased π^* backdonation and relative weakening of the CO bond. The results

require that at least one thermodynamically favored low coordination μ^1 binding site continues to be available in clusters with n up to at least 40 (as we are only dealing here with monocarbonyl complexes, a single favored site is sufficient).

The dominance of atop binding on the late transition metal cluster-monocarbonyl cluster complexes in contrast to CO adsorbed on single crystal surfaces is also attributable to the availability of low coordination sites on the clusters. CO on cobalt, rhodium, and nickel single crystal surfaces often exhibits considerable bridge binding, even, as in the case of Ni(111),³⁰ to the preclusion of atop binding. In the case of vicinal Ni(110) surfaces, ν_{surf} was found to be 2020 cm^{-1} for atop adsorption near step edges, where the metal-metal coordination is lower than on the terraces.³¹ As seen in Fig. 6, the $\nu(\text{CO})$ for the Ni_n cation-CO complexes is tending to a value not far below this ($\nu_{\infty}=2000 \text{ cm}^{-1}$). Thus when the surface presents low coordination sites, the cluster limit is closer to the surface result. The availability of low coordination metal sites has also been used to explain features of CO adsorption on Co nanoparticles supported on alumina³² that are not observed on surfaces, in particular, the ability of single atom sites to accommodate more than one CO molecule. On particles formed following the deposition of Co atoms to an average coverage of 2 Å, $\nu(\text{CO})$ is found to be 1967 cm^{-1} at low coverage. This is 5 cm^{-1} below the Co(10 $\bar{1}$ 0) surface value, but still 25 cm^{-1} above the apparent neutral cluster asymptote (Table I). In this case the CO coverage may still be high enough for the signal to be dominated by CO adsorbed on facets rather than the edge sites.

VI. CONCLUSIONS

A general picture of CO bonding to late transition metal cluster emerges from this work that extends earlier measurements of $\nu(\text{CO})$ on charged and neutral rhodium complexes to larger rhodium clusters and to clusters of cobalt and nickel. Atop binding is ubiquitous in the monocarbonyl complexes, although rhodium cluster complexes also show bridge bonding in certain cases. The size and charge dependences of the C–O stretching frequency can be understood quantitatively in terms of backdonation from the metal to the CO π^* orbital combined with the electrostatic effect of the CO dipole interacting with the charge. Charge dilution is the predominating factor behind the size dependence of $\nu(\text{CO})$ on the charged clusters. At large n , $\nu(\text{CO})$ tends to asymptotes that are not the same as found for $\nu(\text{CO})$ on the single crystal metal surfaces. Instead they converge on the neutral cluster values that are relatively size independent, situated 40–50 cm^{-1} below the single crystal value. This behavior is associated with the availability of lower metal-metal coordinated binding sites on the clusters.

Our results add to the gas phase data that are available as a baseline to gauge the surface induced perturbations in supported clusters. An important parameter in understanding the properties of supported particles, especially their ability to activate chemical bonds, is their charge state. We have already demonstrated how the charge on supported rhodium clusters can be estimated from $\nu(\text{CO})$ using the gas phase results for the corresponding anionic, neutral, and cationic

clusters.¹¹ Such an approach is also feasible for gold cluster-CO complexes.^{12,14} The approximately linear relationship between charge and $\nu(\text{CO})$ established in the earlier work continues to hold for the larger $\text{Rh}_n\text{CO}^{-/0/+}$ complexes and for the $\text{Co}_n\text{CO}^{-/0/+}$ complexes.

Generally, charge will complicate the interpretation of the vibrational spectra of CO adsorbed on deposited metal surfaces of unknown morphology, including metal catalysts where general rules are established to identify the type of binding site from $\nu(\text{CO})$.³³ Small negatively charged clusters in the gas phase have $\nu(\text{CO})$ for atop bound CO well in the range usually associated with bridge binding on single crystal surfaces (2000–1650 cm^{-1}) and certainly below the lowest value normally attributed to atop binding (1950 cm^{-1}). The reference data from the gas phase experiments on particles with defined charged states presented here, in combination with the quantitative model, now provide a gauge for the charging of deposited particles and can thereby give new insights into mechanisms of catalytic reactions involving electron transfer.

ACKNOWLEDGMENTS

We gratefully acknowledge the support of the Stichting voor Fundamenteel Onderzoek der Materie (FOM) in providing beam time on FELIX and the skill of the FELIX staff, in particular, Dr. A. F. G. van der Meer and Dr. B. Redlich.

- ¹J. T. Yates, Jr., T. M. Duncan, S. D. Worley, and R. W. Vaughan, *J. Chem. Phys.* **70**, 1219 (1979).
- ²U. Heiz, A. Sanchez, S. Abbet, and W.-D. Schneider, *Chem. Phys.* **262**, 189 (2000).
- ³B. Yoon, H. Häkkinen, U. Landman, A. S. Wörz, J.-M. Antonietti, S. Abbet, K. Judai, and U. Heiz, *Science* **307**, 403 (2005).
- ⁴M. Frank, R. Kühnemuth, M. Bäumer, and H.-J. Freund, *Surf. Sci.* **427–428**, 288 (1999).
- ⁵M. Frank, R. Kühnemuth, M. Bäumer, and H.-J. Freund, *Surf. Sci.* **454–456**, 968 (2000).
- ⁶M. Frank, M. Bäumer, R. Kühnemuth, and H.-J. Freund, *J. Phys. Chem. B* **105**, 8569 (2001).
- ⁷A. F. Carlsson, M. Naschitzki, M. Bäumer, and H.-J. Freund, *J. Phys. Chem. B* **107**, 778 (2003).
- ⁸G. von Helden, D. van Heijnsbergen, and G. Meijer, *J. Phys. Chem. A* **107**, 1671 (2003).
- ⁹B. Simard, S. Dénoimée, D. M. Rayner, D. van Heijnsbergen, G. Meijer, and G. von Helden, *Chem. Phys. Lett.* **375**, 195 (2002).
- ¹⁰A. Fielicke, G. von Helden, G. Meijer, B. Simard, S. Dénoimée, and D. M. Rayner, *J. Am. Chem. Soc.* **125**, 11184 (2003).
- ¹¹A. Fielicke, G. von Helden, G. Meijer, D. B. Pedersen, B. Simard, and D. M. Rayner, *J. Phys. Chem. B* **108**, 14591 (2004).
- ¹²A. Fielicke, G. von Helden, G. Meijer, D. B. Pedersen, B. Simard, and D. M. Rayner, *J. Am. Chem. Soc.* **127**, 8416 (2005).
- ¹³A. Fielicke, G. von Helden, G. Meijer, B. Simard, and D. M. Rayner, *Phys. Chem. Chem. Phys.* **7**, 3906 (2005).
- ¹⁴A. Fielicke, G. von Helden, G. Meijer, B. Simard, and D. M. Rayner, *J. Phys. Chem. B* **109**, 23935 (2005).
- ¹⁵T. D. Jaeger, A. Fielicke, G. von Helden, G. Meijer, and M. A. Duncan, *Chem. Phys. Lett.* **392**, 409 (2004).
- ¹⁶A. Fielicke, A. Kirilyuk, C. Ratsch, J. Behler, M. Scheffler, G. von Helden, and G. Meijer, *Phys. Rev. Lett.* **93**, 023401 (2004).
- ¹⁷A. Fielicke, C. Ratsch, G. von Helden, and G. Meijer, *J. Chem. Phys.* **122**, 091105 (2005).
- ¹⁸D. Oepets, A. F. G. van der Meer, and P. W. van Amersfoort, *Infrared Phys. Technol.* **36**, 297 (1995).
- ¹⁹G. Blyholder, *J. Phys. Chem.* **68**, 2772 (1964).
- ²⁰J. C. Campuzano, in *The Chemical Physics of Solid Surfaces and Heterogeneous Catalysis*, edited by D. A. King and D. P. Woodruff (Elsevier, Amsterdam, 1990), Vol. 3A, pp. 389–460.

- ²¹E. K. Parks, K. P. Kerns, and S. J. Riley, *J. Chem. Phys.* **112**, 3384 (2000).
- ²²A. J. Lupinetti, S. Fau, G. Frenking, and S. H. Strauss, *J. Phys. Chem. A* **101**, 9551 (1997).
- ²³A. S. Goldman and K. Krough-Jespersen, *J. Am. Chem. Soc.* **118**, 12159 (1996).
- ²⁴M. B. Hall and R. F. Fenske, *Inorg. Chem.* **11**, 1619 (1972).
- ²⁵E. J. Baerends and P. Ros, *Mol. Phys.* **30**, 1735 (1975).
- ²⁶P. S. Braterman, *Metal Carbonyl Spectra* (Academic, London, 1975).
- ²⁷J. P. K. Doye and D. J. Wales, *New J. Chem.* **22**, 733 (1998).
- ²⁸Y.-C. Bae, V. Kumar, H. Osanai, and Y. Kawazoe, *Phys. Rev. B* **72**, 125427 (2005).
- ²⁹M. Zhou, L. Andrews, and C. W. Bauschlicher, Jr., *Chem. Rev. (Washington, D.C.)* **101**, 1931 (2001).
- ³⁰L. Surnev, Z. Xu, and J. T. Yates, Jr., *Surf. Sci.* **201**, 1 (1988).
- ³¹K. Sinniah, H. E. Dorsett, and J. E. Reutt-Robey, *J. Chem. Phys.* **98**, 9018 (1993).
- ³²A. F. Carlsson, M. Bäumer, T. Risse, and H.-J. Freund, *J. Chem. Phys.* **119**, 10885 (2003).
- ³³N. Sheppard and T. T. Nguyen, in *Advances in Infrared and Raman Spectroscopy*, edited by R. E. Hester and R. J. H. Clark (Heyden, London, 1978), Vol. 5, p. 67.
- ³⁴R. L. Toomes and D. A. King, *Surf. Sci.* **349**, 1 (1996).
- ³⁵L.-W. H. Leung, J.-W. He, and D. W. Goodman, *J. Chem. Phys.* **93**, 8328 (1990).
- ³⁶A. M. de Jong and J. W. Niemantsverdriet, *J. Chem. Phys.* **101**, 10126 (1994).
- ³⁷D. H. Wei, D. C. Skelton, and S. D. Kevan, *Surf. Sci.* **381**, 49 (1997).
- ³⁸R. Linke, D. Curulla, M. J. P. Hopstaken, and J. W. Niemantsverdriet, *J. Chem. Phys.* **115**, 8209 (2001).
- ³⁹M. Kawai and J. Yoshinobu, *Surf. Sci.* **368**, 239 (1996).